Dequalinium: A Novel, High-affinity Blocker of CNGA1 Channels

Tamara Rosenbaum,[1] León D. Islas,[2,3] Anne E. Carlson,[2] and Sharona E. Gordon[1,2]

[1]Departments of Ophthalmology, [2]Physiology and Biophysics, and [3]Bioengineering, University of Washington, Seattle, WA 98195

ABSTRACT Cyclic nucleotide–gated (CNG) channels have been shown to be blocked by diltiazem, tetracaine, polyamines, toxins, divalent cations, and other compounds. Dequalinium is an organic divalent cation which suppresses the rat small conductance Ca^{2+}-activated K^+ channel 2 (rSK2) and the activity of protein kinase C. In this study, we have tested the ability of dequalinium to block CNGA1 channels and heteromeric CNGA1+CNGB1 channels. When applied to the intracellular side of inside-out excised patches from *Xenopus* oocytes, dequalinium blocks CNGA1 channels with a $K_{1/2} \approx 190$ nM and CNGA1+CNGB1 channels with a $K_{1/2} \approx 385$ nM, at 0 mV. This block occurs in a state-independent fashion, and is voltage dependent with a $z\delta \approx 1$. Our data also demonstrate that dequalinium interacts with the permeant ion probably because it occupies a binding site in the ion conducting pathway. Dequalinium applied to the extracellular surface also produced block, but with a voltage dependence that suggests it crosses the membrane to block from the inside. We also show that at the single-channel level, dequalinium is a slow blocker that does not change the unitary conductance of CNGA1 channels. Thus, dequalinium should be a useful tool for studying permeation and gating properties of CNG channels.

KEY WORDS: dequalinium • block • CNG channels

INTRODUCTION

CNG channels are important mediators in the visual and olfactory transduction pathways. They are also present in a variety of other tissues where they likely function to facilitate Ca^{2+} entry (for reviews see Zagotta and Siegelbaum, 1996; Richards and Gordon, 2000). In vertebrates, there are at least six different CNG channel subunit genes, with homology between subtypes ranging from ~30–70%. Although some types of CNG channel subunits can form functional homomultimeric channels when expressed in a heterologous system, in vivo they appear to be constructed as heterotetramers, composed of two to three different types of subunits per channel complex (Bonigk et al., 1999; Weitz et al., 2002; Zheng et al., 2002; Zhong et al., 2002). With six membrane-spanning domains, intracellular NH_2 and COOH termini, and conservation in the pore region, CNG channels belong in the superfamily of voltage-gated ion channels, even though they are not activated by voltage alone (Jan and Jan, 1990).

For more than two decades, CNG channels have been known to be blocked by divalent cations such as Ca^{2+} and Mg^{2+} (Haynes et al., 1986; Colamartino et al., 1991; Zimmerman and Baylor, 1992; Root and MacKinnon, 1993; Eismann et al., 1994; Park and MacKinnon, 1995). Both Ca^{2+} and Mg^{2+} are permeant blockers: they traverse the channel but at a much slower rate than Na^+ and K^+ ions (Capovilla et al., 1983; Hodgkin et al., 1985; Torre et al., 1987; Nakatani and Yau, 1988). Recently, the channel was also shown to be blocked by the polycationic polyamines putrescine, spermidine, and spermine from both the extracellular and intracellular sides of the membrane (Lu and Ding, 1999). Thus, four types of ion channels (inward-rectifier K^+, glutamate-gated, acetylcholine-receptor, and CNG channels) are blocked by intracellular and/or extracellular polyamines (Mayer et al., 1984; Nowak et al., 1984; Mathie et al., 1990; Rock and MacDonald, 1992; Lopatin et al., 1994; Koh et al., 1995).

Another blocker of CNG channels is pseudechetoxin (PsTx), a peptide purified from the venom of the Australian king brown snake. When applied to the extracellular face of membrane patches containing homomeric CNGA2 channels, PsTx blocks the cGMP-dependent current. PsTx also blocks homomeric CNGA1 channels with high affinity, but is less effective on the native combination of CNGA1 plus CNGB1 found in rod photoreceptors (Brown et al., 1999).

Finally, local anesthetics are also effective at blocking a wide variety of ion channels (Hille, 2001). Tetracaine has moderate affinity for the native rod channel (Schnetkamp, 1987, 1990; Ildefonse and Bennett, 1991; Quandt et al., 1991). Fodor et al. (1997a,b) demonstrated that high affinity binding of tetracaine to the intracellular surface of CNGA1 and CNGA2 channels occurs only when the pore is in the closed conformation. In addition, two compounds related in structure to tetracaine, L-cis-diltiazem and amiloride, have been shown to block CNG channels (Koch and Kaupp, 1985; Schnetkamp, 1987, 1990; Ildefonse and Bennett, 1991; Quandt et al., 1991; Haynes, 1992; McLatchie and Matthews, 1992, 1994).

Dequalinium is a bis-quinolinium blocker (see Fig. 1 for structure), which blocks the rat small conductance

Address correspondence to Sharona E. Gordon, Department of Ophthalmology, University of Washington, Seattle, WA 98195. Fax: (206) 685-5290; E-mail: seg@u.washington.edu

J. Gen. Physiol. © The Rockefeller University Press • 0022-1295/2003/01/37/11 $8.00
Volume 121 January 2003 37–47
http://www.jgp.org/cgi/doi/10.1085/jgp.20028716

Ca^{2+}-activated K^+ channel 2 (rSK2 channel) when applied to the extracellular surface. It blocks native SK channels in sympathetic neurons (Dunn et al., 1996) as well as recombinant SK channels (Strobaek et al., 2000) with a $K_D \approx 600$ nM. In this study we show that dequalinium chloride is a high-affinity blocker ($K_D \approx 190$ nM at 0 mV) of the rod CNGA1 channel, and nearly as effective on heteromeric CNGA1+CNGB1 channels. By using different cGMP concentrations to activate the channels, as well as the partial agonist cIMP, we show that dequalinium chloride is a state-independent channel blocker and that block of the channel occurs in a voltage-dependent manner. Moreover, single-channel recordings demonstrate that dequalinium induces the appearance of long closed states consistent with the mechanism of action of a slow blocker.

MATERIALS AND METHODS

RNA and Oocytes

DNA for CNGA1 was a gift from Dr. William N. Zagotta. DNA for the human rod subunit 2b of CNGB1 (hRCNC2b) was a gift from Dr. King-Wai Yau (Chen et al., 1993). cRNA was synthesized in vitro, using a standard in vitro transcription kit (mMessage mMachine; Ambion). Segments of ovary were removed from anesthetized *Xenopus laevis*. After gross mechanical isolation, individual oocytes were defolliculated by incubation with collagenase 1A (1 mg/ml) in Ca^{2+}-free OR2 medium (82.5 mM NaCl, 2.5 mM KCl, 1 mM $MgCl_2$, 5 mM HEPES, pH 7.6) for 1.5–3 h. The cells were then rinsed and stored in frog Ringer's solution (96 mM NaCl, 2 mM KCl, 1.8 mM $CaCl_2$, 1 mM $MgCl_2$, 5 mM HEPES, pH 7.6) at 14°C. Oocytes were injected with 50 nL cRNA solution within 2 d of harvest. Electrophysiological recordings were performed 2–10 d after injection.

Current Recording

Inside-out and outside-out patch-clamp recordings were made using symmetrical low divalent NaCl/HEPES/EDTA solutions consisting of 130 mM NaCl, 3 mM HEPES, and 200 μM EDTA (pH 7.2), with cGMP added to the intracellular solution only. Knock-off experiments with inside-out patches were performed to determine whether the blocker interacts with the permeant ion. In this case, the pipette solution was replaced with one containing 13 mM NaCl, 247 mM N-methyl-D-glucamine, 3 mM HEPES, and 200 μM EDTA. The solution bathing the intracellular surface (inside-out configuration) or extracellular surface (outside-out configuration) of the patch was changed using an RSC-200 rapid solution changer (Molecular Kinetics). Dequalinium chloride was prepared as follows: a 0.5 M dequalinium chloride stock was diluted in water and final dequalinium chloride dilutions were made using the low divalent solution described above in the presence of different cGMP concentrations. All chemicals were purchased from Sigma-Aldrich.

Currents were low pass-filtered at 2 kHz and sampled at 10 kHz with an Axopatch 200B (Axon Instruments, Inc.). Data were acquired and analyzed with PULSE data acquisition software (Instrutech) and were plotted and fitted using Igor Pro (Wavemetrics, Inc.). For each experiment, currents in response to low and high concentrations of cGMP were monitored for several minutes and further experimentation did not proceed until these values had stabilized. This was necessary because of a "run up" in the fractional activation by cGMP that occurs after patch excision, and has been shown previously to represent dephosphorylation of the channels by endogenous patch-associated phosphatases (Gordon et al., 1992; Molokanova et al., 1997). All currents shown are difference currents in which the current in the patch in the absence of cyclic nucleotide has been subtracted. In the case of outside-out patches, leak currents were not subtracted. All dose-response curves to dequalinium chloride or to cGMP were measured with a protocol in which the blocker and/or agonist were applied to the patch at a voltage of 0 mV. Since at this voltage the net current flux in our solutions is zero, the patches were held at 0 mV, and stepped to 20 mV for 20 ms at an interval of 5 s. Current measurements with 2 mM cGMP were obtained in the presence of 1 μM $NiCl_2$ in order to obtain maximum open-probability; Ni^{2+} stabilizes the open state of these channels (Gordon and Zagotta, 1995),

All recordings where performed at room temperature. Smooth curves shown in dose-response relations to dequalium chloride are fits with the Hill equation:

$$I = I_{max}\frac{[cGMP]^n}{K_{0.5}^n + [cGMP]^n}. \quad (1)$$

To obtain voltage-current relations, the patches were stepped from a holding potential of 0 mV to between −60 and 80 mV in increments of 20 mV for 15 s until steady-state of block was reached. Block vs. voltage data were fit with the Boltzmann equation:

$$\frac{I_{Deq}}{I_{max}} = \frac{1}{\exp[z\delta(V - V_{0.5})/(kT)]}, \quad (2)$$

where z is the valence of the blocker (two for dequalinium), δ is the electrical distance of the blocker in the pore, T is the absolute temperature, and k is Boltzmann's constant. Data are plotted, unless indicated otherwise, as the fractional current obtained by dividing the blocked current by the maximum unblocked current and reported as the mean ± SEM.

Single Channel Recording

The inside-out configuration of the patch clamp was used for recording of single CNG channels (Hamill et al., 1981). Pipettes were pulled from borosilicate glass and the access resistance was 8–12 MΩ in the recording solution. The bath and pipette solution were the same and had the composition: 130 mM NaCl, 10 mM HEPES, 10 mM EGTA, pH 7.2.

For activation of CNG channels, 2 mM cGMP was added to the recording solution and applied to the inside of the membrane patch with an automatic solution changer through the bore of a 0.5-mm thick capillary. Recordings were acquired using the same instrumentation as described for macroscopic currents. A voltage-clamp pulse to the test voltage was applied from a holding potential of 0 mV for 2 s. Leak subtraction was done using the average of at least 15 null sweeps, obtained in the absence of cGMP. Kinetic analysis was done with TacFit software (Bruxton Co.) and Igor Pro (WaveMetrics, Inc.). Event detection was performed using the 50% threshold crossing method and compiled in the form of log-duration histograms. Fitting of sums of exponential functions was done using maximum-likelihood methods (Sigworth and Sine, 1987). Since at 2 mM cGMP the channel open probability is ≅ 1, recordings were considered to arise from a single channel when no overlapping opening events were observed.

RESULTS

Dequalinium Blocks CNGA1 and CNGA1+CNGB1 Channels

In this study, we have examined the effects of dequalinium (see Fig. 1 A for structure) on CNGA1 channels.

CNGA1 channels were expressed in *Xenopus* oocytes and currents from inside-out patches were obtained. The effect of 1 μM dequalinium (Fig. 1 A) on CNGA1 currents induced by 2 mM cGMP (a saturating concentration) is shown in Fig. 1. Fig. 1 B (left) shows currents obtained in the presence of 2 mM cGMP. The addition of 1 μM dequalinium to this patch effectively induced a nearly complete block of the current flowing through the channels (Fig. 1 B, right). Dequalinium block of these channels reversed with a slow time course (unpublished data).

To obtain an accurate value of the $K_{1/2}$ of block of CNGA1 channels by dequalinium, we performed measurements of the amount of fractional block induced by various dequalinium concentrations in the presence of 2 mM cGMP. Because dequalinium block of these channels was voltage dependent (see below) we wanted to determine the apparent affinity for dequalinium without considering voltage as a factor. We therefore designed a protocol to measure the dequalinium dose-response relation at 0 mV. At 0 mv there was no driving force for current in our symmetrical NaCl solutions. Thus, we held the patches at 0 mV, but at 5-s intervals stepped briefly to 20 mV in order to produce a driving force for current. Because these steps to 20 mV were so brief and the on rate for dequalinium at 20 mV is so slow, these experiments essentially yield a dose-response relation for block by dequalinium at 0 mV. Furthermore, we wanted to begin our study using conditions of maximum open probability. To achieve this we included 1 μM $NiCl_2$ in our bath solution (Gordon and Zagotta, 1995; Sunderman and Zagotta, 1999). The dose-response relation measured under these conditions is shown in Fig. 1 C. Data were fit with Eq. 1, giving a $K_{1/2}$ of 189 nM for block by dequalinium.

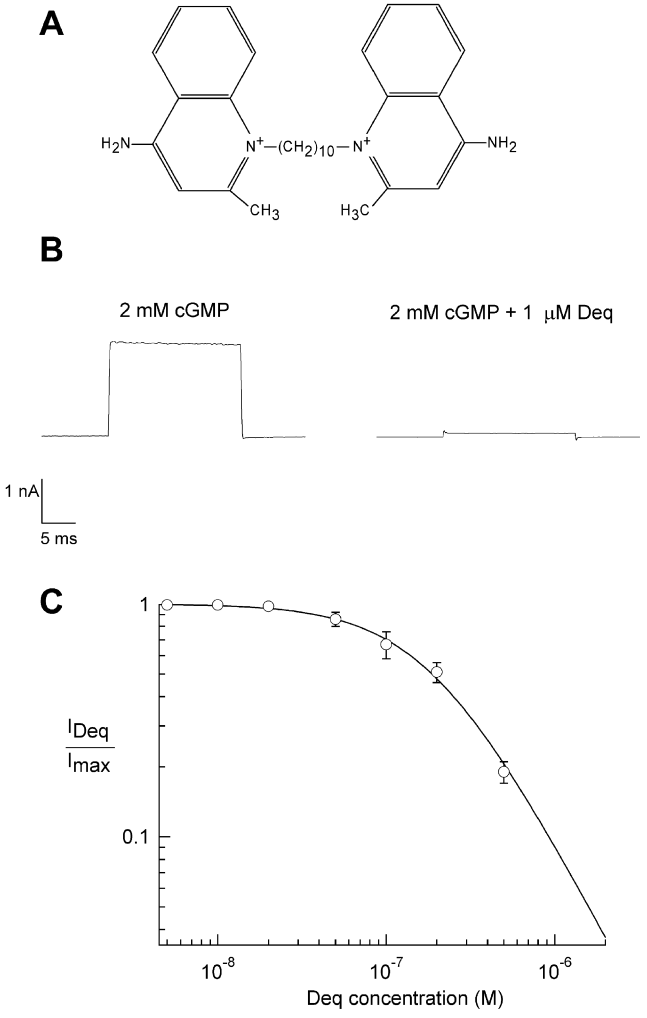

FIGURE 1. Dequalinium blocks CNGA1 channels at a saturating cGMP concentration. (A) Chemical structure of dequalinium (quinolinium, 1,1′-(1, 10-decanediyl)bis(4-amino-2-methyl dichloride)). (B, left) Initial current obtained in the presence of 2 mM cGMP. (B, right) Block of current obtained from the same patch in the presence of 1 μM dequalinium. (C) Dose-response relation for dequalinium block. The smooth curve is a fit with the Hill equation (see MATERIALS AND METHODS) with $K_{1/2}$ = 189 nM and the Hill coefficient = 1.4. All currents were measured at 20 mV. Error bars represent SEM; n = 5 patches.

Because native rod channels are heteromers composed of CNGA1 and CNGB1 subunits in combination, we examined the efficacy of dequalinium on channels expressed from a 1:4 mixture of CNGA1 and CNGB1 RNA (Shammat and Gordon, 1999). We found that dequalinium was also an effective blocker of these heteromeric channels, giving a $K_{1/2}$ for block of 385 nM at 0 mV (Fig. 2).

Dequalinium Block of CNGA1 Channels Is Asymmetric

We further examined the ability of dequalinium to block CNGA1 channels by applying the blocker to the extracel-

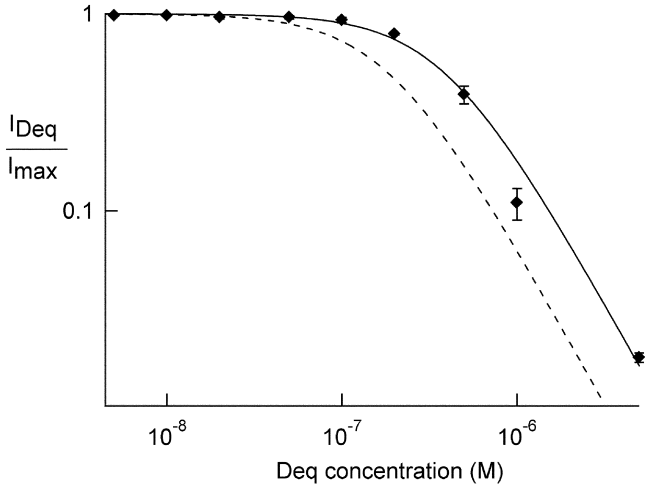

FIGURE 2. Dequalinium blocks heteromeric CNGA1+CNGB1 channels. Dose-response relation for block of heteromeric channels by dequalinium. A 1:4 ratio of CNGA1:CNGB1 RNA was injected in oocytes. The dotted curve was taken from the CNGA1 homomeric data shown in Fig. 1 C. Data from heteromeric channels (diamonds) were fit with the Hill equation with the following parameters: $K_{1/2}$ = 385 nM, Hill coefficient = 1.5.

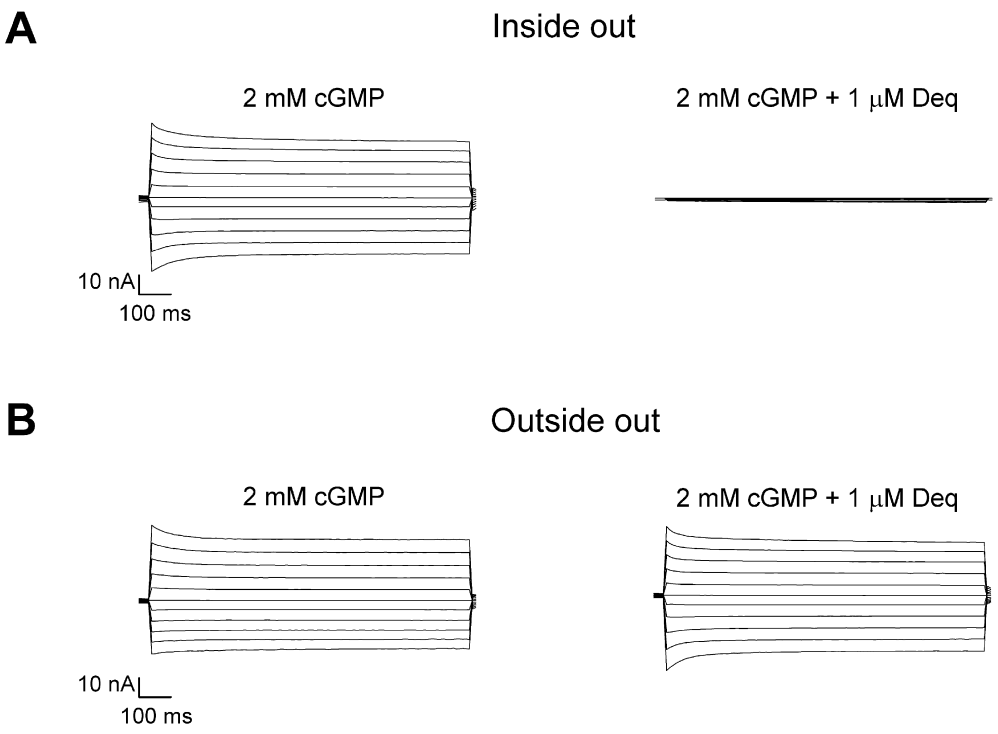

FIGURE 3. Block of cGMP-activated currents by dequalinium is more effective from the intracellular side of the channels. (A and B) Current families were recorded in response to voltage steps from 0 mV to between −100 and 100 mV in 20-mV steps. (A) Currents recorded in the inside-out configuration in the absence (left) and presence of 1 μM dequalinium (right). (B) Currents recorded in the outside-out configuration in the absence (left) and presence of 1 μM dequalinium (right).

lular side of the channels. For this purpose we performed the same experiments described above but using the outside-out configuration of the patch-clamp technique. Fig. 3 shows a comparison of dequalinium block from the inside to dequalinium block from the outside. Fig. 3 A, left, shows currents obtained in the presence of 2 mM cGMP at different voltages. When 1 μM dequalinium was applied to this inside-out patch, currents were completely blocked (Fig. 3 A, right). In this case we did not wait the very long time necessary for unblock at hyperpolarized potentials, leading to apparent block at all potentials examined. In contrast, when the same concentration of dequalinium was applied to an outside-out patch, it had almost no effect on currents at all voltages (Fig. 3 B, right). It should be noted that in Fig. 3 A, right, we applied dequalinium for only a short period of time and obtained nearly complete block in the inside-out configuration, whereas almost no block was attained in the outside-out configuration (Fig. 3 B, right). The currents shown in Fig. 3, A and B, right, are not at steady-state, due to the considerable difference in the time constants for internal block compared with external block, and the slow kinetics of unblock at all voltages.

To compare differences in the kinetics of dequalinium block when applied to the intracellular versus extracellular surface of the channels, we plotted the time course of block for both types of experiment in Fig. 4 A. Block by 1 μM dequalinium applied to the intracellular surface of a patch reached steady-state in around 2 min (open symbols). In contrast, when dequalinium was applied to the extracellular surface of a patch, block was not reached, even after 19 min of exposure to dequalinium (closed symbols). Half-block by 1 μM dequalinium in the outside-out configuration could only be attained if the patch was in the presence of dequalinium for >25 min (as in Fig. 4 A, filled circles).

We wondered whether the slow time course observed when applying dequalinium from the outside might reflect slow diffusion of dequalinium across the membrane. If this were the case, a sufficient concentration of dequalinium might accumulate over time at the intracellular side of the channels. The block we observe then, even though we applied dequalinium to the extracellular surface, might actually occur by dequalinium present at the intracellular surface. To test this hypothesis we examined the voltage dependence of dequalinium block from the outside. If dequalinium binds to a region at the extracellular end of the pore then it should be driven into the channels when the holding potential is stepped from 0 mV to a hyperpolarized potential. In contrast, if dequalinium diffuses across the membrane to block from the inside, then block should be augmented by steps to depolarizing potentials. Results from one such experiment are shown in Fig. 4 B. Here we used 2 mM cGMP in the pipette to activate the channels in this outside-out patch. We applied 1 μM dequalinium to the extracellular surface of the patch and stepped the voltage from a holding potential of 0 to 100 mV followed by a step to −100 mV before stepping the potential back to 0 mV. As can be seen in the figure, dequalinium block was greatly augmented during the voltage pulse to 100 mV and was relieved during the voltage pulse to −100 mV.

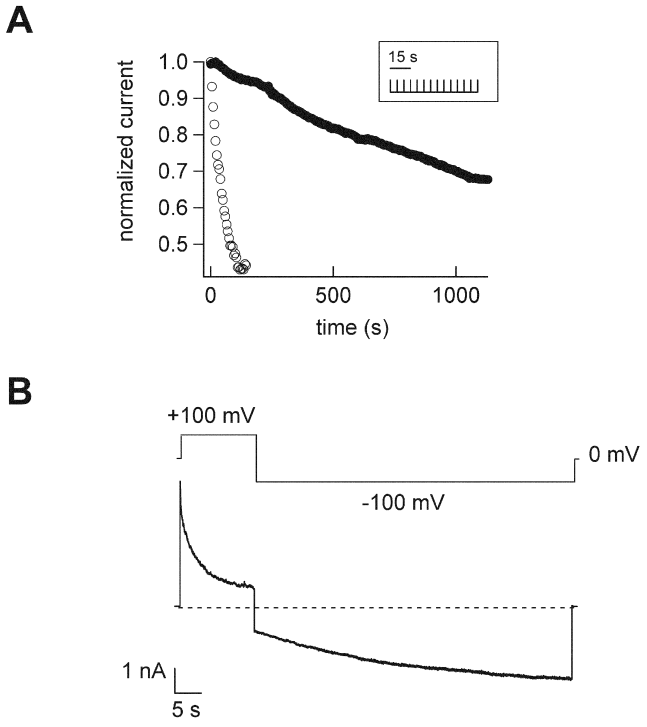

FIGURE 4. Dequalinium applied to the extracellular surface appears to block from the inside. (A) Time-course for block by 1 μM dequalinium applied to the intracellular surface of an inside-out patch (open symbols) and 1 μM dequalinium applied to the extracellular surface of an outside-out patch (filled circles). Each time course was fit with a single exponential, with a $\tau = 53$ ms for the inside-out patch and $\tau = 1{,}429$ ms for the outside-out patch. The inset represents the voltage protocol used for these experiments. (B) Current response to a voltage protocol, as indicated above the data. Here, 1 μM dequalinium was applied to the extracellular surface of an outside out patch. The current decay at 100 mV indicates block and the relaxation at −100 mV represents unblock.

This block at a depolarized potential and unblock at a hyperpolarized potential are predicted by the model in which dequalinium applied to the extracellular surface permeates through the membrane to block from the intracellular side.

Block of CNGA1 Channels by Dequalinium Is State Independent

We examined whether the apparent affinity of the channels for dequalinium was influenced by the activation state of the channels. Fig. 5 A compares the dose-response relation for dequalinium block in the presence of a saturating cGMP concentration where most of the channels were open (2 mM cGMP + 1 μM Ni^{2+}; open circles, same data as in Fig. 1 C) to the dequalinium dose-response relation in the presence of a subsaturating (32 μM) cGMP concentration in which about half of the channels were open (squares). The $K_{1/2}$ for both cGMP concentrations was ~190 nM (Hill fit, solid line). This suggests that the binding of the blocker to the channel occurred in a state-independent fashion.

We also performed experiments measuring the dose-response for activation by cGMP in the absence and presence of a fixed concentration of dequalinium (400 nM). In Fig. 5 B, filled symbols represent the dose-response relation for activation by cGMP in the absence of dequalinium ($K_{1/2} = 90$ μM), whereas empty symbols represent the dose-response for activation by cGMP obtained in the presence of dequalinium ($K_{1/2} = 80$ μM). If dequalinium block were state dependent, we would expect the $K_{1/2}$ for the two cGMP dose-response relations to be different. When the data obtained in the presence of the blocker are normalized to the data obtained in the absence of the blocker, the resulting fit (Hill fit, dotted line) greatly resembles the fit obtained for the data obtained in the absence of the blocker.

To further distinguish between state-dependent and state-independent block we used a simple model for channel activation in which two cyclic nucleotide-binding events are followed by an allosteric conformational change in the pore:

SCHEME I

We used Scheme I to fit the dose–response relation for activation by cGMP in the absence of dequalinium (Fig. 5 C, black curve). We then considered three ways in which dequalinium could interact with the different states of the channel: only with the closed states (Scheme II), only with the open state (Scheme III), or with equal affinity for the open and closed states (Scheme IV):

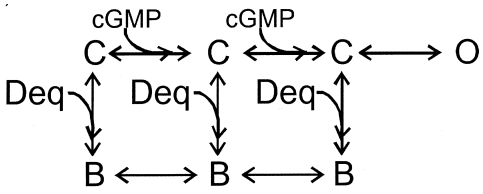

SCHEME II

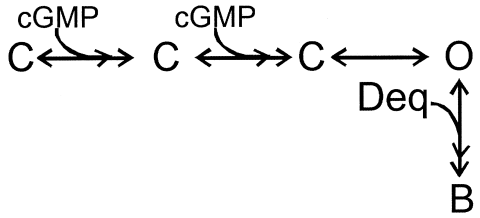

SCHEME III

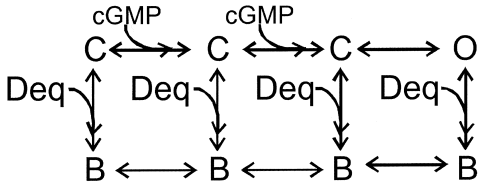

SCHEME IV

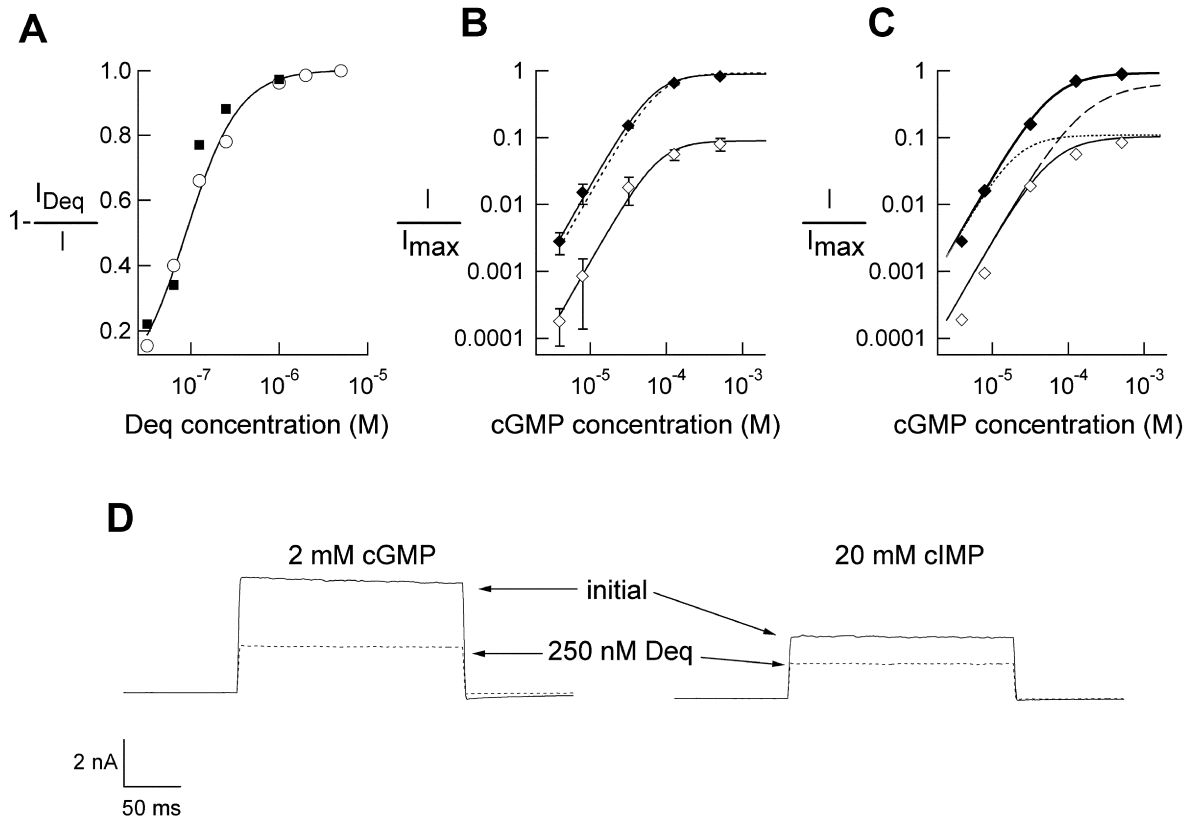

FIGURE 5. Block by dequalinium is state independent. (A) Dose-response relations for dequalinium block in the presence of saturating cGMP (2 mM cGMP, filled squares) and in the presence of subsaturating cGMP (32 μM cGMP, open circles). Data are presented as fraction of block for comparison purposes. The smooth line is a fit with Eq. 1, $K_{1/2}$ = 189 nM. (B) Dose-response for cGMP in the absence (filled diamonds) and presence of 400 nM dequalinium (open diamonds). Error bars represent SEM, n = 4 patches. The smooth lines represent fits to the Eq.1 with $K_{1/2}$ = 80 μM in the presence of dequalinium $K_{1/2}$ = 90 μM in the absence of dequalinium. Dotted line represents normalization of the data obtained in the presence of 400 nM dequalinium to the data obtained in the absence of dequalinium, $K_{1/2}$ = 80 μM. (C) Predicted fits with the models shown in Schemes 1–4. Filled and hollow diamonds are from the same data in B. The dashed line represents a fit with Scheme III (pure open channel block), the dotted line represents block only in the closed state (Scheme II, pure closed channel block) and the thin line represents block occurring equally during the closed and open states of the channel with a K_D = 50 nM for both of the conformational states (Scheme IV). The parameter values for these fits were L = 19 and K = 3800 M^{-1} (in all cases). (D) Block of currents by 250 nM dequalinium in the presence of 2 mM cGMP (left) and in the presence of 20 mM cIMP, a partial agonist of these channels (right). In both cases block was of ~48%.

Fits to each of these schemes to the dose-response relation for activation by cGMP in the presence of a fixed dequalinium concentration (400 nM) are shown in Fig. 5 C. Scheme II, which allows block only of closed channels, fails to fit the data at high cGMP concentrations when the open probability is high (thin curve). Scheme III, which allows dequalinium binding only to the open state, fails to fit the data at low cGMP concentrations when the channel open probability is small (dotted curve). Scheme III, which allows dequalinium binding to both the closed states and the open states can adequately describe the data. As shown by the dashed curve in Fig. 5 C, Scheme IV provides a fit to the data that can accommodate both the points at high and low cGMP concentrations, with a K_D for dequalinium binding of 50 nM for both the open and closed states.

Finally, we used a partial agonist of CNGA1 channels, cIMP, which activated nearly 70% of the current activated by saturating cGMP. When 20 mM cIMP was used, 250 nM dequalinium blocked ~48% of the current (Fig. 5 D, right) similar to what occurred when channels were activated by 2 mM cGMP (Fig. 5 D, left). These data further support the idea that the apparent affinity of CNGA1 channels for dequalinium does not vary with the activation state of the channels.

Voltage Dependence of Dequalinium Block

To examine the voltage dependence of dequalinium block, we recorded from CNGA1 channels in the presence of 2 mM cGMP and 400 nM dequalinium at different voltages. Fig. 6 A, right, shows representative traces from a patch exposed to dequalinium at −60 and 60

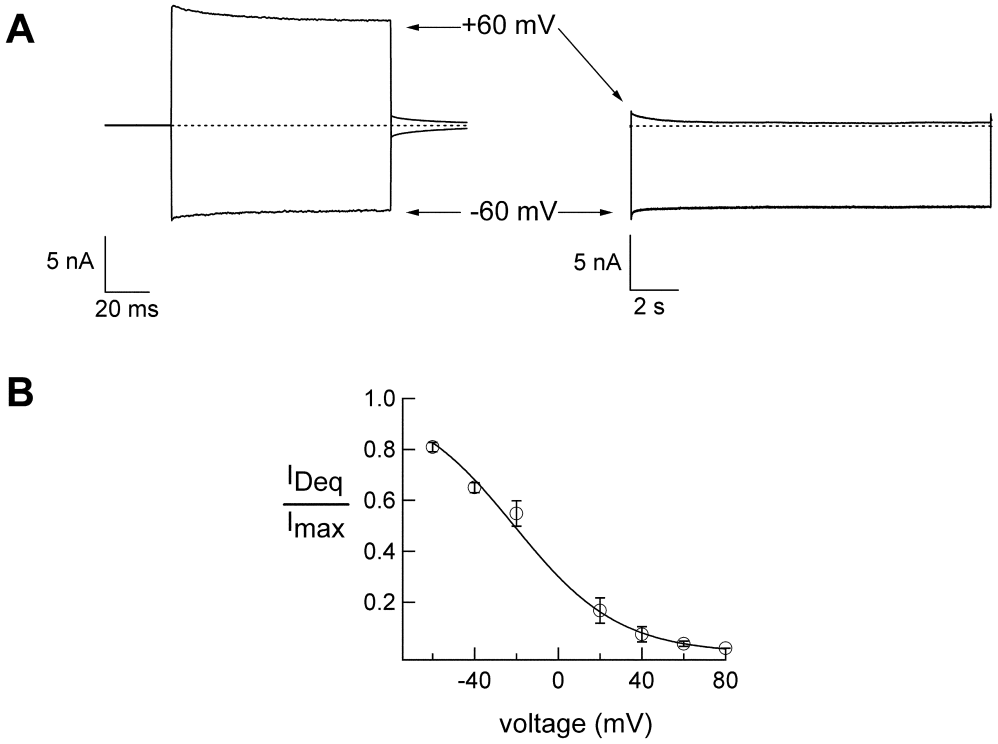

FIGURE 6. Voltage dependence of dequalinium block. (A) Current traces obtained at −60 and 60 mV (as indicated by the arrow) in the absence of dequalinium (left) and in the presence of 400 nM dequalinium (right). Dashed line marks the zero current level. (B) Current-voltage relation obtained from holding at the different voltages indicated until steady-state was reached. The smooth curve represents a fit with Eq. 2 with a value of $z\delta$ =

mV as indicated by the arrows. When compared with currents in the absence of dequalinium (left), a dramatic block of current at positive potentials, but not negative potentials, was observed when the blocker was applied. Since the data in the right-hand panel were obtained with a sample frequency of 500 Hz, the fast component of voltage-dependent block was not resolved. The data shown in Fig. 6 A are consistent with the idea that dequalinium binds to a site within the membrane electric field. Fig. 6 B illustrates the voltage dependence of dequalinium block in these channels by plotting I_{Deq}/I_{max} versus voltage for a range of voltages. The data were fit with the Boltzmann equation (solid line; see MATERIALS AND METHODS). The equivalent charge $z\delta$ obtained by the fit to this equation was 1.

To further test the hypothesis that dequalinium binds within the pore, we designed an experiment to address whether it interacts with the permeant ions: a knock-off experiment using asymmetric ionic conditions. In these experiments, the bath solution (internal solution) contained 130 mM NaCl while the pipette solution (external solution) contained 13 mM NaCl and the osmolarity and ionic strength were balanced with an impermeant cation, N-methyl-D-glucamine. Under these conditions of reduced permeant cation, occupancy of the pore by the blocker should be increased. Indeed, the data shown in Fig. 7 demonstrate that this is true for dequalinium. Here the dose-response for block by dequalinium with symmetric ionic conditions (Fig. 7, A and B, dashed line) are compared with the dose-response for block by dequalinium with these asymmetric ionic conditions (Fig. 7 B, triangles). The shift to the left of the dose-response relation measured with our asymmetric solutions indicates that the apparent affinity of the channels for dequalinium did indeed increase. The $K_{1/2}$ of block obtained using asymmetric solutions was 40 nM, compared with 190 nM in symmetrical ionic conditions. These data support the hypothesis that dequalinium interacts with the permeant ion, probably because it occupies a binding site in the pore.

Single Channel Blockade by Dequalinium

We found that single CNG channels activated by 2 mM cGMP showed gating characteristics comparable to what others have observed (Haynes et al., 1986; Bucossi et al., 1997; Ruiz and Karpen, 1999; Sunderman and Zagotta, 1999). Under these conditions, activation is almost saturated and the open probability was not noticeably voltage dependent (0.92 at −60 mV vs. 0.94 at 60 mV); the single channel I-V curve was almost linear with a slight rectification at extreme voltages (unpublished data). Single channel conductance was estimated to be 26.4 pS, from the fit of a line to the I-V relationship.

Fig. 8 A shows recordings of a single CNG channel at 60 mV; the open probability was very high (close to 1). When 5 nM dequalinium was added to the internal solution (Fig. 8, C–H), the current amplitude (upward deflections) did not change, as shown in the all-points amplitude histograms (Fig. 8, D compared with B). In-

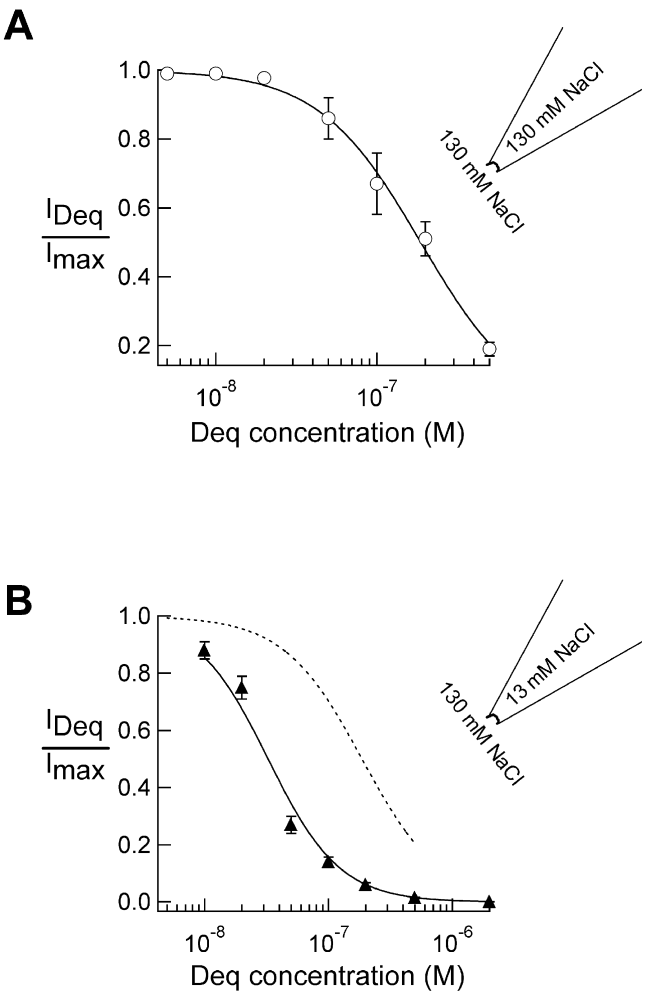

FIGURE 7. Interaction of dequalinium with the permeant ion. (A) Dose-response relation for block by dequalinium in 130 mM NaCl (circles) with $K_{1/2}$ = 189 nM and (B) triangles represent data obtained with 13 mM NaCl with $K_{1/2}$ = 39 nM (knock-off experiment) and the dotted-line represents data shown in A (see MATERIALS AND METHODS). Error bars represent SEM, n = 5.

stead, a long-lived closed (blocked) state appeared and the number of null traces (traces without channel openings) increased from 0 to 26 from a total of 120. Analysis of the dwell time duration histograms shows that the open state duration was not affected by dequalinium. Open state duration histograms in the presence (Fig. 8 H) and absence (Fig. 8 F) of dequalinium were fitted with the sum of two exponentials, with time constants 3.4 and 16 ms. In contrast, closed time duration in the absence of dequalinium (Fig. 8 E) could be fitted with two exponentials, with time constants 0.3 and 8.4 ms. When dequalinium was added, the relative contribution of the intermediate exponential (7.2 ms) increased from ~1% to ~16% and a third component with time constant 43.7 ms appeared that corresponds to the long blocked periods (Fig. 8 G). These data are consistent with the idea that dequalinium is a slow blocker, with a long-lived dwell time when bound to the pore, that is, a slow OFF rate constant.

DISCUSSION

In this study we demonstrate that dequalinium is a high affinity blocker of CNGA1 channels. Dequalinium exhibits the following characteristics for block of CNGA1 channels: (a) block occurs in a state-independent fashion; (b) it is voltage dependent and happens through a mechanism that involves interaction with the permeant ion; and (c) at the single channel level the appearance of long closed states are observed with no change in unitary conductance.

Block of CNG channels by dequalinium is fundamentally different from block of these channels by tetracaine; tetracaine binds preferentially to the closed state of the channels, and with a 100-fold lower affinity than dequalinium (Fodor et al., 1997a,b). The higher affinity of CNG channels for dequalinium compared with tetracaine can be explained by a slower unblocking rate constant (k_{off}).

Dequalinium exhibits higher affinity for block from the intracellular side of CNGA1 channels compared with the outside, pointing to a structural asymmetry between the external and the internal sides of the channel. This renders dequalinium as a useful tool to perform structural analysis of these channels especially because it lacks the extra complication of state dependence of block. Voltage dependence of block in CNG channels has been shown for other blockers such as tetracaine (Fodor et al., 1997b) and diltiazem (Haynes, 1992; McLatchie and Matthews, 1992, 1994).

The current-voltage relation of block by dequalinium shows that $z\delta = 1$. Since the valence (z) for dequalinium is 2, the data are consistent with block of dequalinium half-way through the pore (Hille, 2001). This explanation holds only if the membrane potential decays linearly in the pore and the dequalinium positive charges are close together, assumptions that are almost certainly untrue. A second possibility is that one of the charges of the molecule traverses the whole length of the channel's pore. It is more likely, however, that the $z\delta$ arises as a combination of an "effective valence" of dequalinium, z', such that $1 < z' < z$ interacting at some distance δ. The fact that block by dequalinium is voltage dependent strongly suggests interaction of the blocker with some region in the pore or alternatively with some region in the protein within the membrane's electric field. A previous study (Spassova and Lu, 1998) has shown that the high voltage sensitivity ($z\delta = 1$) of monovalent blockers in ROMK1 channels is due to coupled movement of one permeant K^+ ion and the blocker. A similar mechanism could be at work in our system.

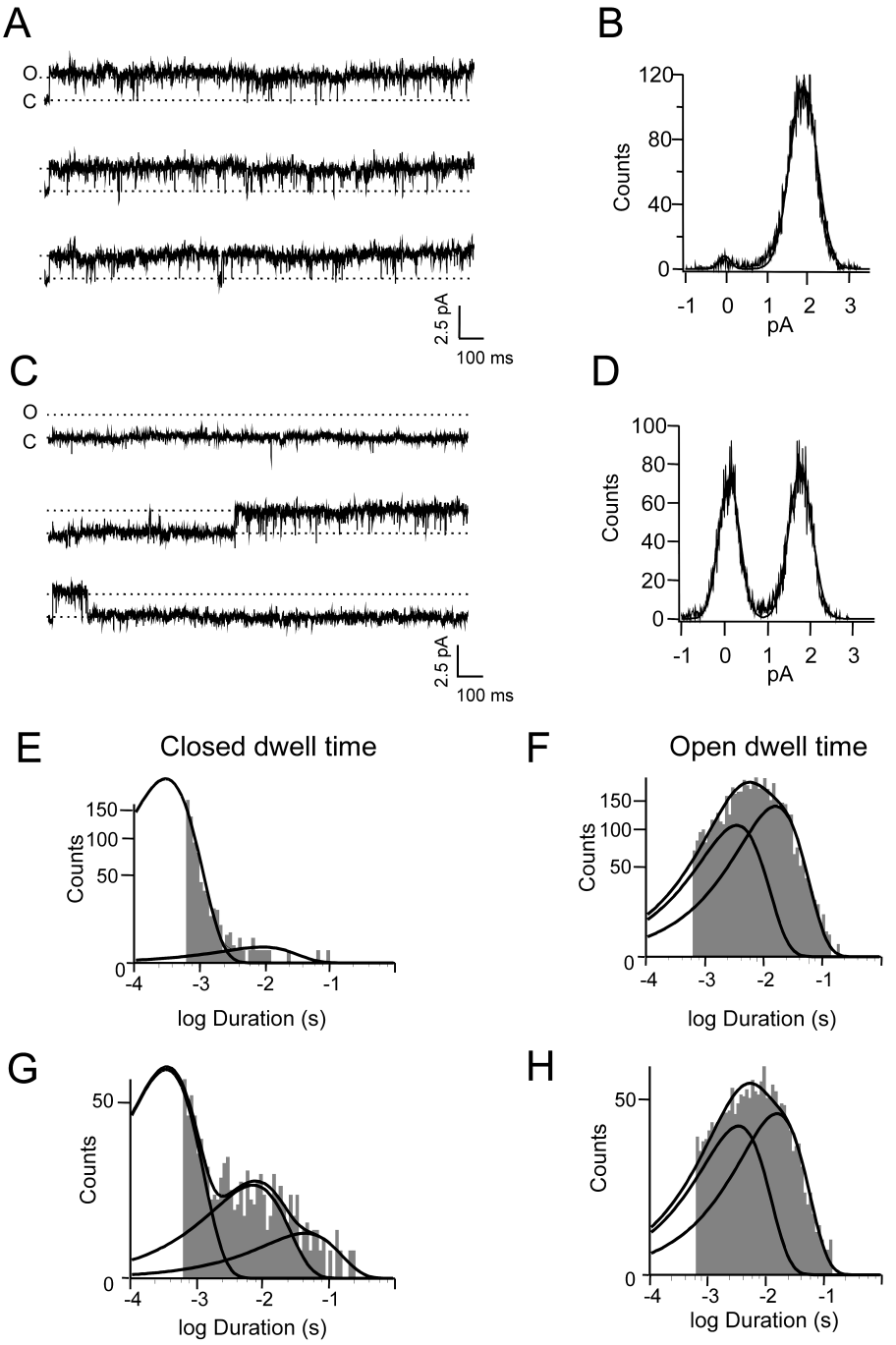

FIGURE 8. Single-channel recordings. (A) Single-channel current traces in response to depolarizing voltage pulses to 60 mV in the presence of 2 mM cGMP. Channel open probability = 0.92. Open (O) and closed (C) levels are indicated in the figure. (B) All-points amplitude histogram that corresponds to a current amplitude of 1.9 pA. (C) Current traces from the same channel in A recorded in the presence of 5 nM dequalinium at the same potential. (D) The amplitude histogram shows that the single-channel conductance remains unchanged. (E) The closed distribution for cGMP alone can be fit with sum of two exponentials of time constants 0.34 and 8.4 ms. (F) Open time constant for cGMP alone. The distribution can be fitted with sums of two exponentials with time constants 3.4 and 16 ms. (G) Closed time distribution in the presence of 5 nm dequalinium. In the presence of dequalinium the same time constants are present (0.35 and 7.2 ms), but a third (43.7 ms) appears that corresponds to the blocked state. (H) Open time distribution in the presence of 5 nM dequalinium. The distribution can be fitted with sums to two exponentials (3.4 and 15.6 ms). Similar results were obtained from three other single-channel patches.

Single channel recordings indicate that dequalinium acts as a slow blocker. It promotes the appearance of long closed states (with no change in unitary conductance) rather than promoting "flickering" between the closed and open states which would be characteristic of a fast (low affinity) blocker (Hille, 2001). High-affinity blockers of other channels, such TTX for sodium channels and charybdotoxin and TEA for potassium channels, have provided fascinating mechanistic information on how these channels function (Hille, 1975; Anderson et al., 1988; MacKinnon and Miller, 1988, 1999). Dequalinium should prove to be a similar tool for CNG channels.

The apparent affinity of open and closed channels for dequalinium are indistinguishable, as demonstrated by the data shown in Fig. 5 where the $K_{1/2}$ for the dequalinium dose responses in saturating and subsaturating cGMP are equal and the percentage of block by a given dequalinium concentration in the presence of 2 mM cGMP or in the presence of 20 mM cIMP (a partial agonist of CNGA1 channels) is the same. This state independence is a unique property among high-

affinity CNG channel blockers. Dequalinium's state-independence raises the question of how a blocker interacting with the pore—which is known to change conformations during activation—can have such high affinity, reflecting quite an intimate interaction with its binding site, and yet not appear to "sense" the change in conformation? The answer to this question is important to providing further insights into the mechanism of activation in CNG channels.

We thank Dr. William N. Zagotta for his kind gift of the CNGA1, Mika Munari for expert technical assistance, and Drs. Marcos Rosenbaum and Li Hua for proofreading this manuscript.

Supported in part by National Institutes of Health grants R01 EY13007 and EY01730, and in part by an unrestricted grant from Research to Prevent Blindness, Inc. S.E. Gordon is a Jules and Doris Stein RPB Professor.

Olaf Andersen served as editor.

Submitted: 13 September 2002
Revised: 3 December 2002
Accepted: 3 December 2002

REFERENCES

Anderson, C.S., R. MacKinnon, C. Smith, and C. Miller. 1988. Charybdotoxin block of single Ca2+-activated K+ channels. Effects of channel gating, voltage, and ionic strength. *J. Gen. Physiol.* 91:317–333.

Bonigk, W., J. Bradley, F. Muller, F. Sesti, I. Boekhoff, G.V. Ronnett, U.B. Kaupp, and S. Frings. 1999. The native rat olfactory cyclic nucleotide-gated channel is composed of three distinct subunits. *J. Neurosci.* 19:5332–5347.

Brown, R.L., T.L. Haley, K.A. West, and J.W. Crabb. 1999. Pseudechetoxin: a peptide blocker of cyclic nucleotide-gated ion channels. *Proc. Natl. Acad. Sci. USA.* 96:754–759.

Bucossi, G., M. Nizzari, and V. Torre. 1997. Single-channel properties of ionic channels gated by cyclic nucleotides. *Biophys. J.* 72: 1165–1181.

Capovilla, M., A. Caretta, L. Cervetto, and V. Torre. 1983. Ionic movements through light-sensitive channels of toad rods. *J. Physiol.* 343:295–310.

Chen, T. Y., Y.W. Peng, R.S. Dhallan, B. Ahamed, R.R. Reed, and K.W. Yau. 1993. A new subunit of the cyclic nucleotide-gated cation channel in retinal rods. *Nature.* 363:764–767.

Colamartino, G., A. Menini, and V. Torre. 1991. Blockage and permeation of divalent cations through the cyclic GMP-activated channel from tiger salamander retinal rods. *J. Physiol.* 440:189–206.

Dunn, P.M., D.C. Benton, J. Campos Rosa, C.R. Ganellin, and D.H. Jenkinson. 1996. Discrimination between subtypes of apamin-sensitive Ca(2+)-activated K+ channels by gallamine and a novel bis-quaternary quinolinium cyclophane, UCL 1530. *Br. J. Pharmacol.* 117:35-42.

Eismann, E., F. Muller, S.H. Heinemann, and U.B. Kaupp. 1994. A single negative charge within the pore region of a cGMP-gated channel controls rectification, Ca2+ blockage, and ionic selectivity. *Proc. Natl. Acad. Sci. USA.* 91:1109–1113.

Fodor, A.A., K.D. Black, and W.N. Zagotta. 1997a. Tetracaine reports a conformational change in the pore of cyclic nucleotide-gated channels. *J. Gen. Physiol.* 110:591–600.

Fodor, A.A., S.E. Gordon, and W.N. Zagotta. 1997b. Mechanism of tetracaine block of cyclic nucleotide-gated channels. *J. Gen. Physiol.* 109:3–14.

Gordon, S.E., D.L. Brautigan, and A.L. Zimmerman. 1992. Protein phosphatases modulate the apparent agonist affinity of the light-regulated ion channel in retinal rods. *Neuron.* 9:739–748.

Gordon, S.E., and W.N. Zagotta. 1995. Subunit interactions in coordination of Ni2+ in cyclic nucleotide-gated channels. *Proc. Natl. Acad. Sci. USA.* 92:10222–10226.

Hamill, O.P., A. Marty, E. Neher, B. Sakmann, and F.J. Sigworth. 1981. Improved patch-clamp techniques for high-resolution current recording from cells and cell-free membrane patches. *Pflugers Arch.* 391:85–100.

Haynes, L.W. 1992. Block of the cyclic GMP-gated channel of vertebrate rod and cone photoreceptors by l-cis-diltiazem. *J. Gen. Physiol.* 100:783–801.

Haynes, L.W., A.R. Kay, and K.W. Yau. 1986. Single cyclic GMP-activated channel activity in excised patches of rod outer segment membrane. *Nature.* 321:66–70.

Hille, B. 1975. Ionic selectivity, saturation, and block in sodium channels. A four-barrier model. *J. Gen. Physiol.* 66:535–560.

Hille, B. 2001. Ion channels of excitable membranes. Sinauer Associates.

Hodgkin, A.L., P.A. McNaughton, and B.J. Nunn. 1985. The ionic selectivity and calcium dependence of the light-sensitive pathway in toad rods. *J. Physiol.* 358:447–468.

Ildefonse, M., and N. Bennett. 1991. Single-channel study of the cGMP-dependent conductance of retinal rods from incorporation of native vesicles into planar lipid bilayers. *J. Membr. Biol.* 123:133–147.

Jan, L.Y., and Y.N. Jan. 1990. A superfamily of ion channels. *Nature.* 345:672.

Koch, K.W., and U.B. Kaupp. 1985. Cyclic GMP directly regulates a cation conductance in membranes of bovine rods by a cooperative mechanism. *J. Biol. Chem.* 260:6788–6800.

Koh, D.S., N. Burnashev, and P. Jonas. 1995. Block of native Ca(2+)-permeable AMPA receptors in rat brain by intracellular polyamines generates double rectification. *J. Physiol.* 486:305–312.

Lopatin, A.N., E.N. Makhina, and C.G. Nichols. 1994. Potassium channel block by cytoplasmic polyamines as the mechanism of intrinsic rectification. *Nature.* 372:366–369.

Lu, Z., and L. Ding. 1999. Blockade of a retinal cGMP-gated channel by polyamines. *J. Gen. Physiol.* 113:35–43.

MacKinnon, R., and C. Miller. 1988. Mechanism of charybdotoxin block of the high-conductance, Ca2+-activated K+ channel. *J. Gen. Physiol.* 91:335–349.

MacKinnon, R., and C. Miller. 1989. Mutant potassium channels with altered binding of charybdotoxin, a pore-blocking peptide inhibitor. *Science.* 245:1382–1385.

Mathie, A., D. Colquhoun, and S.G. Cull-Candy. 1990. Rectification of currents activated by nicotinic acetylcholine receptors in rat sympathetic ganglion neurones. *J. Physiol.* 427:625–655.

Mayer, M.L., G.L. Westbrook, and P.B. Guthrie. 1984. Voltage-dependent block by Mg2+ of NMDA responses in spinal cord neurones. *Nature.* 309:261–263.

McLatchie, L.M., and H.R. Matthews. 1992. Voltage-dependent block by L-cis-diltiazem of the cyclic GMP-activated conductance of salamander rods. *Proc. R. Soc. Lond. B Biol. Sci.* 247:113–119.

McLatchie, L.M., and H.R. Matthews. 1994. The effect of pH on the block by L-cis-diltiazem and amiloride of the cyclic GMP-activated conductance of salamander rods. *Proc. R. Soc. Lond. B Biol. Sci.* 255:231–236.

Molokanova, E., B. Trivedi, A. Savchenko, and R.H. Kram. 1997. Modulation of rod photoreceptor cyclic nucleotide-gated channels by tyrosine phosphorylation. *J. Neurosci.* 17:9068–9076.

Nakatani, K., and K.W. Yau. 1988. Calcium and magnesium fluxes across the plasma membrane of the toad rod outer segment. *J.*

Physiol. 395:695–729.

Nowak, L., P. Bregestovski, P. Ascher, A. Herbet, and A. Prochiantz. 1984. Magnesium gates glutamate-activated channels in mouse central neurons. *Nature.* 307:462–465.

Park, C.S., and R. MacKinnon. 1995. Divalent cation selectivity in a cyclic nucleotide-gated ion channel. *Biochemistry.* 34:13328–13333.

Quandt, F.N., G.D. Nicol, and P.P. Schnetkamp. 1991. Voltage-dependent gating and block of the cyclic-GMP-dependent current in bovine rod outer segments. *Neuroscience.* 42:629–638.

Richards, M.J., and S.E. Gordon. 2000. Cooperativity and cooperation in cyclic nucleotide-gated ion channels. *Biochemistry.* 39: 14003–14011.

Rock, D.M., and R.L. Macdonald. 1992. The polyamine spermine has multiple actions on N-methyl-D-aspartate receptor single-channel currents in cultured cortical neurons. *Mol. Pharmacol.* 41:83–88.

Rock, D.M., and R.L. MacDonald. 1992. Spermine and related polyamines produce a voltage-dependent reduction of N-methyl-D-aspartate receptor single-channel conductance. *Mol. Pharmacol.* 42:157–164.

Root, M.J., and R. MacKinnon. 1993. Identification of an external divalent cation-binding site in the pore of a cGMP-activated channel. *Neuron.* 11:459–466.

Ruiz, M., and J.W. Karpen. 1999. Opening mechanism of a cyclic nucleotide-gated channel based on analysis of single channels locked in each liganded state. *J. Gen. Physiol.* 113:873–895.

Schnetkamp, P.P. 1987. Sodium ions selectively eliminate the fast component of guanosine cyclic 3′,5′-phosphate induced Ca2+ release from bovine rod outer segment disks. *Biochemistry.* 26: 3249–3253.

Schnetkamp, P.P. 1990. Cation selectivity of and cation binding to the cGMP-dependent channel in bovine rod outer segment membranes. *J. Gen. Physiol.* 96:517–534.

Shammat, I.M., and S.E. Gordon. 1999. Stoichiometry and arrangement of subunits in rod cyclic nucleotide-gated channels. *Neuron.* 23:809–819.

Sigworth, F.J., and S.M. Sine. 1987. Data transformations for improved display and fitting of single-channel dwell time histograms. *Biophys. J.* 52:1047–1054.

Spassova, M., and Z. Lu. 1998. Coupled ion movement underlies rectification in an inward-rectifier K+ channel. *J. Gen. Physiol.* 112:211–221.

Strobaek, D., T.D. Jorgensen, P. Christophersen, P.K. Ahring, and S.P. Olesen. 2000. Pharmacological characterization of small-conductance Ca(2+)-activated K(+) channels stably expressed in HEK 293 cells. *Br. J. Pharmacol.* 129:991–999.

Sunderman, E.R., and W.N. Zagotta. 1999. Mechanism of allosteric modulation of rod cyclic nucleotide-gated channels. *J. Gen. Physiol.* 113:601–620.

Torre, V., G. Rispoli, A. Menini, and L. Cervetto. 1987. Ionic selectivity, blockage and control of light-sensitive channels. *Neurosci. Res. Suppl.* 6:S25–S44.

Weitz, D., N. Ficek, E. Kremmer, P.J. Bauer, and U.B. Kaupp. 2002. Subunit stoichiometry of the CNG channel of rod photoreceptors. *Neuron.* 36:881–889.

Zagotta, W.N., and S.A. Siegelbaum. 1996. Structure and function of cyclic nucleotide-gated channels. *Annu. Rev. Neurosci.* 19:235–263.

Zheng, J., M.C. Trudeau, and W.N. Zagotta. 2002. Rod cyclic nucleotide-gated channels have a stoichiometry of three CNGA1 subunits and one CNGB1 subunit. *Neuron.* 36:891–896.

Zhong, H., L.L. Molday, R.S. Molday, and K.W. Yau. 2002. The heteromeric cyclic nucleotide-gated channel adopts a 3A:1B stoichiometry. *Nature.* 420:193–198.

Zimmerman, A.L., and D.A. Baylor. 1992. Cation interactions within the cyclic GMP-activated channel of retinal rods from the tiger salamander. *J. Physiol.* 449:759–783.